Laser Light Scattering Study on the Structure of a Poly(vinylidene fluoride) Aggregate in the Dilute Concentration State

Il Hyun Park,* Jeong Eun Yoon, Yong Chul Kim, Ling Yun, and Sang Cheol Lee

Department of Polymer Science and Engineering, Kumoh National Institute of Technology, Kumi, Kyungbuk 730-701, Republic of Korea

Received October 21, 2003

ABSTRACT: By means of laser light scattering, poly(vinylidene fluoride) (PVDF) chains were found to form complex aggregates of very narrow size distribution even at dilute concentrations of good solvents such as propylene carbonate (PC) and γ-butyrolactone (BL). Almost the same radii of gyration for aggregates in both solvents were obtained as $R_G \sim 220 \pm 10$ nm. Their static sizes appeared to be concentration-independent as well as temperature-independent at a wide temperature range of 25−160 °C in each solvent. As for solvent effects, the static scattering intensities had different scattering patterns especially at high-q regimes and also different hydrodynamic radii were observed as $R_H = 380 \pm 10$ nm in propylene carbonate and $R_H = 320 \pm 10$ nm in γ-butyrolactone, respectively. By the introduction of both core−shell structure and core size distribution, the intensity patterns of scattered light and large ratios of R_H/R_G could be explained. The attractive inter-/intramolecular force between four consecutive sequences of head-to-tail CF_2 groups was proposed as a driving force, and the amount of head-to-head configuration in PVDF chain seemed to have strong relation with the size of the aggregate.

Introduction

Since many scientists have been recently interested in thermoreversible physical gels as one of the new fields of macromolecular science,[1,2] the nature and structure of physical gels have been extensively investigated by means of various experimental techniques[1] and theoretical approaches[3−8] but there are still some controversial and unsolved topics especially for the physical gelation of the crystalline polymer.[1]

As one of the interesting crystalline polymers, poly(vinylidene fluoride) (PVDF) is chosen in this study because of optical transparency as well as its well-known piezoelectric and pyroelectric properties. It was first reported by Cho et al.[9] in 1993 that the PVDF/γ-butyrolactone system was a transparent, thermoreversible gel. Later Nandi et al.[10−14] systematically investigated the physical gelation of PVDF in a wide range of temperatures and concentrations in various solvents such as acetophenone, ethyl benzoate, and glyceryl tributyrate. According to their reports, gelation could occur even at very low gel formation concentration, C_{gel} of ∼1 wt %, and the gelation time, t_{gel}, could be scaled with ϕ^n. Here the reduced overlapping concentration ϕ is defined as $[C - C_{gel}(T)]/C_{gel}(T)$ at a solution temperature T.

To clearly understand thermoreversible gelation of a crystalline PVDF polymer, more careful investigation is necessary because conformation change sometimes accompanies gelation. Around C_{gel}, the polymer becomes usually milky and then laser light scattering can be no longer an effective research tool. However, as above mentioned, our systems such as PVDF/propylene carbonate (PC) and PVDF/γ-butyrolactone (BL) have two advantages: (i) very low C_{gel} (=(1−2) × 10^{-2} g/mL), which is ∼10 times lower than other gelation systems; (ii) transparent gels due to close matching of refractive indices between polymer and solvents. In this respect, this system is considered as a suitable one to study the gelation mechanism by means of laser light scattering.

Table 1. Physical Properties of the Poly(vinylidene fluoride) Sample

MW (nominal)	534 000 g/mol (from Aldrich)
melt viscosity	27.9 kP at 230 °C
melt index	5 g/10 min at 230 °C and 12.5 kg
intrinsic viscosity	78.1 mL/g (in DMAC[a] at 130 °C)
melting point	163.5 °C
heat of fusion	6.69, 5.95 kJ/mol
crystallinity	38.7 wt % (from 6.69 kJ/mol)
mole ratio of head-to-head[b]	∼5.9%

[a] DMAC = *N*,*N*-dimethylacetamide. [b] It is defined as ((B7 + C7 + E7)/3)/A7 for simple estimation.

Our original objective was to elucidate how PVDF chain conformation changes and how the structure of thermoreversible gel develops as approaching gel formation concentration at a given temperature. However, according to our previous study,[15] at room temperature PVDF chains of the pregel state existed as very large but monodisperse aggregates of $R \sim 0.4$ μm instead of freely separated chains. In addition, other literatures[9,14,34] about PVDF gel had reported that the gel morphology had been developed by piling up lots of spheres of 0.2−0.8 μm radius range. To explain these observations, conformation change should occur at a certain concentration.

To confirm this aggregation, more systematic experiment is surely necessary. Thus, in this paper the following things will be discussed in more detail: (i) concentration, temperature, and solvent dependence of the aggregate static and hydrodynamic size; (ii) the core−shell model as a possible structure of the aggregate; (iii) a driving force in this aggregation process.

Experimental Section

Materials. Poly(vinylidene fluoride) (Aldrich, catalog no. 18270-2) of the nominal molecular weight MW = 534 kg/mol was used in this experiment, and other physical properties of this sample were listed in Table 1. Since it was difficult to

* To whom correspondence should be addressed. E-mail: ilhyunpark@hanmail.net.

10.1021/ma030534v CCC: $27.50
Published on Web 07/16/2004

find a powerful solvent dissolving PVDF up to freely separated chains in solution without formation of complex aggregate, the melt viscosity (27.9 kP at 230 °C) and melt index were also listed in Table 1 for estimation of molecular weight. And the intrinsic viscosity of this sample was measured as $[\eta] = 78.1$ mL/g at 130 °C in *N*,*N*-dimethylacetamide. However, although Aldrich had supplied melt viscosity data at 230 °C and GPC data (M_w, M_n) for several PVDF samples without description of the details of GPC experimental conditions, the empirical relation between melt viscosity (η_m; poise unit) and weight average molecular weight could be set up as $\eta_m = 8.2 \times 10^{-3} M_w^{1.15}$, $r = 0.93$. At this equation, the exponent of 1.15 appeared to be a little larger than the unity value of the Rouse model perhaps because of the polydispersity of these samples. The melting temperature T_m was determined as 163.5 °C with a duPont 910 DSC at a heating rate of 10 °C/min under a nitrogen atmosphere, and its crystallinity was obtained as about 38.7 wt %. This PVDF sample had also some irregular head-to-head configuration of ~5.9% compared to head-to-tail configuration, and the refractive index of PVDF ($n_D^{25} \sim 1.41$) was so close to that of propylene carbonate ($n_D^{25} = 1.4199$, Sigma-Aldrich, HPLC grade) or γ-butyolactone ($n_D^{25} = 1.4348$, Sigma-Aldrich) that a light scattering experiment was able to be done near the gelation point. These solvents were also used after treatment with dehydrating agent or molecular sieves (4A) for a while.

Light Scattering. Our homemade laser light scattering instrument was equipped with Brookhaven detector, Brookhaven digital correlator (model BI-9000AT), and Ar-ion laser (Lexel model 95) operated with the $\lambda_o = 514$ nm line. As a container of refractive index (RI) matching oil, the vat was made of just one piece of precision Pyrex tube (diameter 94 mm) without any junction seal so it could be heated to very elevated temperatures of above 160 °C. The light scattering (LS) cell holder (o.d. 75 mm) was immersed into the RI matching oil and was designed for bath fluid to circulate from the outside hot oil bath into the inside of the cell holder. And by circulating again this fluid around the outside cylindrical bronze body supporting the vat, the temperature gradient between the inside and the outside of the vat was minimized especially for high-temperature measurement. True solution temperature was indirectly estimated from the temperature of matching oil, after setting up the relation between two temperatures of solution inside the LS cell and of matching oil in the vat. For a heat-exchanging bath fluid and RI matching oil, a high-quality silicone oil (Cole-Parmer Silicone 200/20 or Silicone 710) was used in this experiment. The detailed design of the light scattering spectrometer has been described elsewhere.[16]

The *z*-average characteristic line width $\langle\Gamma\rangle$ was analyzed by the second-order cumulant method.[17] The effective hydrodynamic radius R_H was calculated from the *z*-average translational diffusion constant D_o using the Stokes−Einstein equation:[18]

$$D_o = (\langle\Gamma\rangle/q^2)_{C=0,q=0} = k_B T/6\pi\eta_o R_H \quad (1)$$

Here q ($=4\pi n_o \sin(\theta/2)/\lambda_o$), k_B, and η_o are the magnitude of scattering vector, Boltzmann constant, and solvent shear viscosity, respectively. For calculation of R_H at high temperature, shear viscosities of PC and BL were carefully measured up to ~150 °C by our calibrated Ubbelohde type viscometer and the relations of temperature dependence were given as

$$\eta_o = 1.0311 \times 10^{-2} \exp(1634.5/T)$$
solvent, PC; units, cP, K (2)

$$\eta_o = 1.840 \times 10^{-2} \exp(1355.2/T)$$
solvent, BL; units, cP, K (3)

At $\lambda_o = 514$ nm and 40 °C, the specific increment of refractive index, d*n*/d*C*, was also obtained as −0.012 mL/g for PVDF/PC and −0.029 mL/g for PVDF/BL, respectively. Such small values supported again that these were relatively good refractive index matching systems. Prior to our experiment, the possibility of Mie scattering was checked through its rough criterion of $4\pi R(m-1)/\lambda \geq 1$, where R is radius of the particle and m is the ratio of refractive index of the particle to that of the solvent. Since this criterion value of our system was calculated as ~0.15 with $R \sim 380$ nm, the possibility of Mie scattering was excluded and only Rayleigh−Debye scattering was considered in this study.

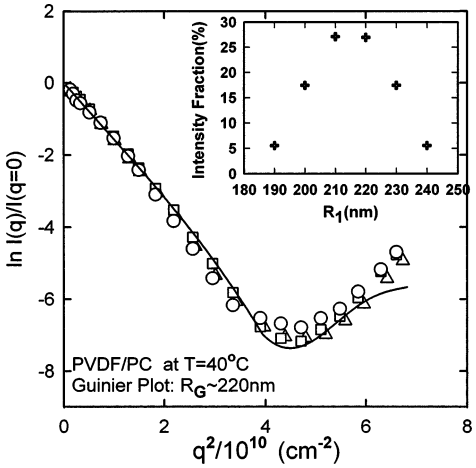

Figure 1. Plot of ln $I(q)/I(q = 0)$ vs q^2 at several different concentrations and $T = 40$ °C in PVDF/PC system. The solid line stands for the calculated $P(q)$ with $x = 0.07$, $C_R = 0.1$, and the core size distribution shown in the inserted graph. Other symbol notations: (triangles) $C = 0.016$ wt %; (squares) $C = 0.045$ wt %; (circles) $C = 0.168$ wt %.

For light scattering experiment, optically clean (i.e. dust-free) polymer mother solution was obtained by the centrifuging method (4000 rpm, 30 min at 25 °C) instead of filtration method because the membrane filter was easily clogged due to large aggregate particles of submicrometer order. After centrifuging of the mother polymer solution of ~0.3 wt %, change of concentration was corrected with the differential refractometer. Since this solution had the long-term effect of precipitation, we tried to finish measurements within ~12 h after preparation and for next day measurement the solution was heated again for 1 h at ~90 °C.

Results and Discussion

Static Light Scattering. As it is well-known that PVDF solution forms thermoreversible gels in many solvents[9−15,19] such as propylene carbonate (PC), γ-buyrolactone (BL), acetophenone, and ethyl benzoate, light scattering experiments were carried out at two systems of PVDF/PC and PVDF/BL to get some idea of chain conformation in the pregel state of $C \ll C_{gel}$. The concentration range used in this study was about 0.01−0.168 wt %, and the lowest concentration corresponds to about 1/100 of C_{gel} (≈1 wt %).[19] The pattern of normalized scattered intensity $I(q)/I(q = 0)$ was analyzed to investigate dependence on experimental conditions such as polymer concentration, solution temperature and solvent. From Figures 1 and 2, the following things have been observed: (i) Instead of s Zimm plot,[20] a Guinier plot[21] should be use to determine the radii of gyration of the particles. Actually, this means that our particles are not single polymer chains but huge aggregates. (ii) Almost the same radii of gyration R_G's of these aggregates are obtained at 220 nm for both solvents. The scattered intensity patterns and the radii of gyration seem to be concentration- and temperature-independent at least in PC and BL solutions as shown in Figures 1 and 2. (iii) However, the scattered intensity pattern at high-q^2 range and the first minimum position,

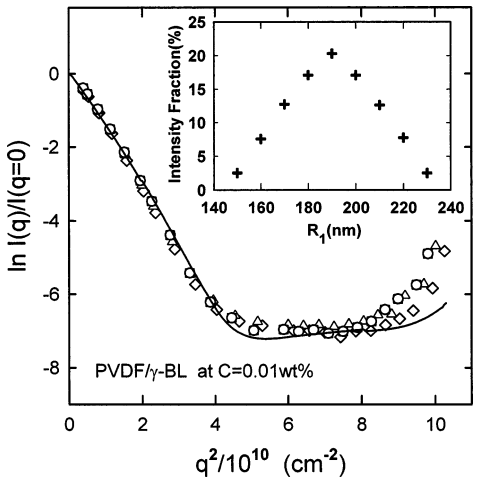

Figure 2. Plot of ln $I(q)/I(q = 0)$ vs q^2 at several different temperatures and $C = 0.01$ wt % in PVDF/BL system. The solid line stands for the calculated $P(q)$ with $x = 0.15$, $C_R = 0.1$, and the core size distribution shown in the inserted graph. Other symbol notations: (diamonds) 26.8 °C; (triangles) 70.7 °C; (squares) 109 °C; (circles) 158 °C.

q_{min}, are observed as solvent-dependent. For example, q_{min}^2 is 4.6×10^{10} cm^{-2} for PC solution but is ambiguous due to a flat pattern for BL solution.

Here we tried to estimate the weight-average molecular weight, M_w, and the second virial coefficient, A_2, of this system in the range of $1 \times 10^{-4} < C$ (unit g/mL) $< 1.4 \times 10^{-3}$ in PC solution. They turn out to be approximately $M_w = 4.9 \times 10^8$ g/mol and $A_2 = -2.1 \times 10^{-7}$ (mol mL)/g^2. If Aldrich's nominal molecular weight (534 000 g/mol) can be used as M_w of PVDF chain without any criticism, it is found that each aggregate consists of about 900 chains. Therefore, due to some kind of thermodynamic attractive force of very small negative A_2 (its order of magnitude of 10^{-7}), PVDF chains form large aggregates. We will discuss later where the attractive interaction comes from and what is the driving force.

According to the scattering theory of monodisperse sphere particle,[21−23] the form factor of $P_{sph}(x) = (9/x^6)$-$(\sin x - x \cos x)^2$ with $x \equiv qR$ has many minimums in its scattering function. In our PVDF/PC scattering pattern, observation of minimum q_{min} indicates that our particles may be huge in size but spherelike in shape. As its first minimum position of the above mentioned form factor is well-known as $x = 4.493$,[22,23] other size information can be obtained from the value of q_{min}^2. From $q_{min}^2 \sim 4.6 \times 10^{10}$ cm^{-2} for PVDF/PC, the geometrical radius R is estimated as 208 nm. With $R_G/R = 0.775$ of the homogeneous hard sphere,[20] the radius of gyration calculated from q_{min} should be the order of 160 nm (=0.775 × 208 nm) for a PC solution. So the big difference between R_G's values from the two different methods ($R_G = 220$ nm from the Guinier plot and $R_G = 161$ nm from the q_{min} method) indicates that the structure of our particle is not a homogeneous hard sphere but a more complicated one. A similar type of structure can be also applied to the PVDF/BL system, even though the minimum disappeared and instead the flat pattern was observed as shown in Figure 2. Here it should be also noted that the HV component (i.e. the horizontally polarized scattered intensity for the vertically polarized incident light) was not detected at all. This means that our particles do not have any anisotropic character. The detail structure of this spherical aggregate will be discussed in the next section.

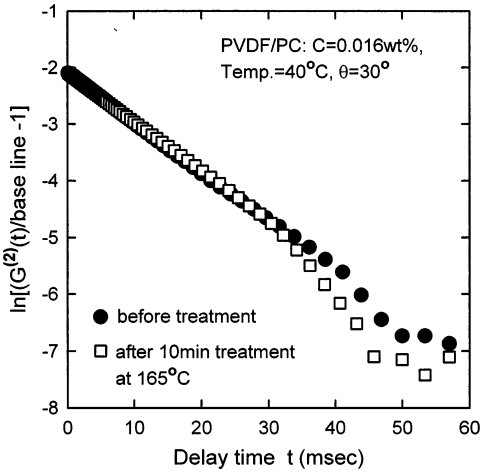

Figure 3. Semilog plot of the normalized $G^{(2)}(\tau)$ versus the delay time τ. After maintenance for 10 min at 165 °C, the second time correlation function was measured again but there was no significant difference between two time correlation functions. The linear relation also means that this sample has a very narrow size distribution.

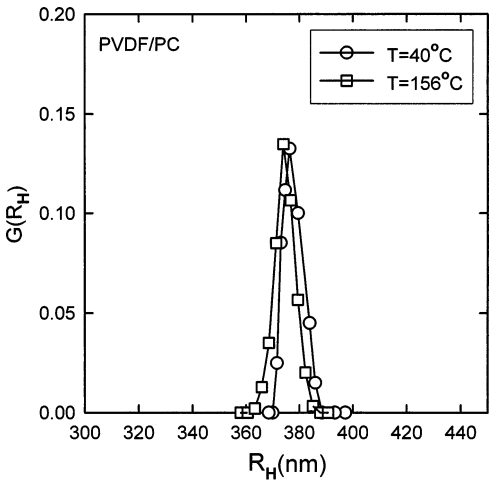

Figure 4. Hydrodynamic size distribution of PVDF aggregate at two different temperatures. There is no significant difference between two size distributions.

Dynamic Light Scattering. The hydrodynamic size and polydispersity of this aggregate can be also estimated from the time correlation function of dynamic light scattering. While the natural logarithm of $G^{(2)}(\tau)$ is plotted against the delay time τ in Figure 3, a very good linear relation supports that this system has a narrow size distribution. To check if there may exist somewhat undissolved PVDF chains, the time correlation function was measured again at 40 °C after being kept for ~10 min about 165°C (melting point of PVDF, 163.5 °C). Since two time correlation functions are almost identical, we can exclude any possibility that some portion of the aggregate consists of undissolved crystalline polymer. Even at elevated temperature, the size distribution is shifted downward by 5−7 nm as shown in Figure 4 but there is actually no temperature dependence within experimental error. Here the size distribution was obtained by means of NNCLS (nonnegatively constrained least squares) analysis method.[24]

At the wide temperature range of 25−156 °C and under a fixed concentration ($C = 0.016$ wt %) of the PVDF/PC system, typical q^2 dependence of $\langle\Gamma\rangle/q^2$ is shown at Figure 5. If this concentration is approximated at a dilute enough condition (see Figure 6), according

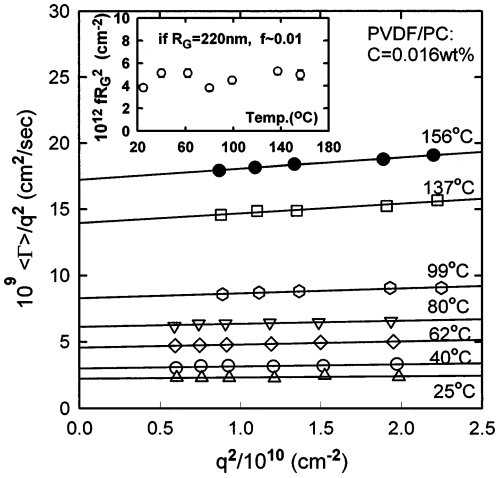

Figure 5. q^2 dependence of $\langle\Gamma\rangle/q^2$ obtained at the various temperatures and the temperature effect of fR_G^2 at a fixed concentration $C = 0.016$ wt % in PVDF/propylene carbonate system. With $R_G \sim 220$ nm, f values have been obtained as ~0.01 and these are much smaller than the random coil's value of 0.17−0.2.

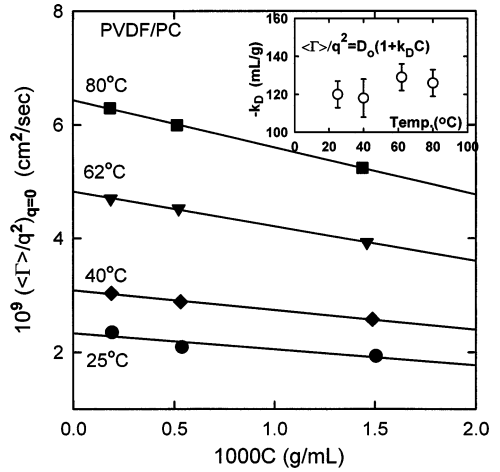

Figure 6. Concentration dependence of $(\langle\Gamma\rangle/q^2)_{q=0}$ at the various temperatures and the temperature dependence of the second virial coefficient k_D of the diffusion constant in the PVDF/propylene carbonate system. As there is an attractive force between aggregate particles, k_D has been obtained as a large negative value.

to the equation $\langle\Gamma\rangle/q^2 = D_o(1 + fR_G^2q^2)$, $(\langle\Gamma\rangle/q^2)/D_o$ was plotted against q^2. And then the slope corresponds to fR_G^2, where f is a polydispersity- and/or structure-dependent parameter.[25] The plot of fR_G^2 vs temperature in Figure 5 has two characteristics: (i) very small f value of ~0.01; (ii) no temperature dependence. According to Burchard,[25] f becomes zero for a monodisperse hard sphere but $f = 0.17-0.20$ for a random coil;[25] thus, it is confirmed again that the aggregated particles consist of spheres of very narrow size distribution.

Next, to see the concentration dependence of $(\langle\Gamma\rangle/q^2)_{q=0}$ through the second virial coefficient k_D of diffusion constant in the equation $(\langle\Gamma\rangle/q^2)_{q=0} = D_o(1 + k_DC)$, $(\langle\Gamma\rangle/q^2)_{q=0}$ has been plotted against C in Figure 6. The k_D of −125 mL/g has been found to be temperature independent and such large negative slope indicates the existence of some kind of attractive force between the particles. However, since k_D is given as $k_D = 2A_2M_w - k_f - \nu_2$, where k_f and ν_2 (~order of 1 mL/g) mean the concentration dependent coefficient of frictional force and the partial specific volume of particle, respectively,[18]

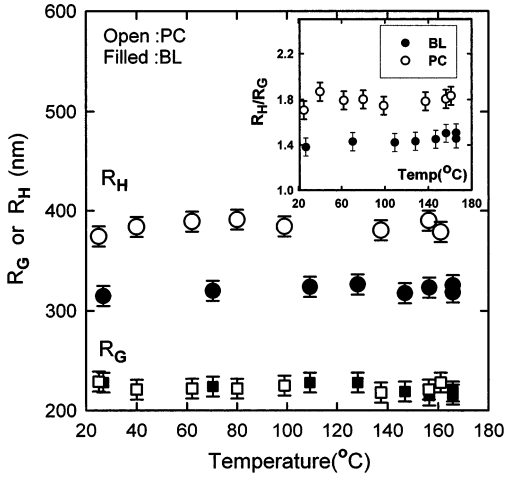

Figure 7. Plots of the hydrodynamic radius R_H, the radius of gyration R_G, and R_H/R_G as a function of solution temperature in two systems of PVDF/γ-buytrolactone (filled symbols) and PVDF/propylene carbonate (open symbols).

the large negative value of k_D comes mainly from the negative A_2 in the term of $2A_2M_w$ ($= -2 \times 2.1 \times 10^{-7} \times 4.9 \times 10^8 = -206$ mL/g). Here if we assume that $(\langle\Gamma\rangle/q^2)_{q=0,C=0.016\text{ wt }\%}$ can approximate the translational diffusion constant D_o $[=(\langle\Gamma\rangle/q^2)_{q=0,C=0}]$ within a few % error, the effective hydrodynamic radii can be obtained quickly from only data of $(\langle\Gamma\rangle/q^2)_{q=0,C=0.016\text{ wt }\%}$ especially above 100 °C, unless the solution becomes yellowish slowly.

If concentration effect is negligible at $C = 0.01$ wt % in PVDF/BL just like in PVDF/PC system, the apparent R_G and R_H are measured at $C = 0.01$ wt % as increasing temperature. All data for R_G and R_H of two different systems are plotted against the solution temperature in Figure 7. Here two interesting results are obtained: (i) no temperature dependence of both R_G and R_H in both solvents; (ii) solvent dependence of R_H (380 nm in PC, 320 nm in BL) unlike solvent independence of R_G (220 nm at least in two solvents of PC and BL).

It is interesting to know if the gel formation concentration of PVDF system can be estimated only with the experimental data for dilute concentration. Under two assumptions that the hydrodynamic radius R_H is regarded as the geometrical radius R and that the gel formation concentration C_{gel} will be the order of the contact concentration C^* $(=3M_w/4\pi R^3N_A)$ of these spheres, C^* is calculated as 1.1×10^{-2} g/mL with $R =$ 380 nm and $M_w = 5 \times 10^8$ g/mol, which is very close to the experimental value of $C_{gel} \sim 1.4 \times 10^{-2}$ g/mL observed by Nandi et al.[10] Thus, we think the gel formation occurs near the contact concentration where the spheres begin to touch each other. It is important to know that these spheres have not formed suddenly near the gel point but have already existed even at very low concentration as a type of conformation of the PVDF chains.

Core−Shell Structure and Solvent Effect. As shown in Figure 7, unexpectedly high R_H/R_G ratios ($R_H/R_G = 1.45-1.8$) are obtained in this study, compared with $R_H/R_G = 1.291$ in hard sphere and $R_H/R_G = 0.78-0.81$ in the Flory Θ solvent.[26] To rationalize this large value, the sphere should have a dense inner part and a loose outer, where the dense core part is responsible mainly for R_G and the outer part for R_H. Here several models for its structure has been surveyed, but no one gives some reasonable features except the core−shell

model. For example, for linearly decreasing density model where the center has the highest density, the value of $R_H/R_G = 1.45-1.8$ is never obtained through eq 4.[23,27]

$$R_G^2 = \int_0^R r^2\rho(r)4\pi r^2\,dr/\int_0^R \rho(r)4\pi r^2\,dr \qquad (4)$$

Thus, the core−shell model is regarded as a simple but plausible one for our aggregate particles. According to Hirzinger et al.,[28] sterically stabilized poly(methyl methacrylate) dispersions had a similar core−shell structure with high R_H/R_G (∼1.7) value. Next we will try to estimate inner core radius R_1 and density ratio x ($=\rho_{shell}/\rho_{core}$) between core and shell. Under nondraining conditions in the shell part, the geometrical radius R can approximate the effective hydrodynamic radius R_H obtained by dynamic light scattering. With two variables of core radius R_1 and density ratio x, iterative calculations with eqs 5 and 6[23] can be applied so as to get the correct scattered intensity pattern:

$$R_G^2 = \frac{3}{5}\left[\frac{R_1^5 + x(R^5 - R_1^5)}{R_1^3 + x(R^3 - R_1^3)}\right] \quad \text{for core−shell model} \qquad (5)$$

$$I(q) = A(q)^2 \cong [\int \rho(r)4\pi r^2(\sin(qr)/qr)\,dr]^2$$

$$A(q) \sim \frac{4\pi\rho_{core}}{q^3}[(1-x)(\sin qR_1 - qR_1\cos qR_1) + x(\sin qR - qR\cos qR)] \quad \text{for core−shell model} \qquad (6)$$

Actually for matching the calculated form factor to the experimental one, two more corrections were introduced for calculation of theoretical $P(q)$. The first correction comes from the contribution of the backward beam reflected at several interfaces. In our light scattering instrument, there exist three different kinds of interfaces such as glass−air, glass−solvent, and glass−matching silicone oil. From the interface of i and j, the reflectance R_{ij} ($=(n_i - n_j)^2/(n_i + n_j)^2$) of the normal beam can be calculated easily with the corresponding refractive indices such as $n_g \sim 1.472$, $n_o \sim 1.475$, $n_s \sim 1.420$, and $n_a \sim 1.000$. Here n_g, n_o, n_s, and n_a stand for the refractive index of glass, of matching oil, of solvent, and of air, respectively. On the basis of the calculated reflectance values of $R_{ga} = 0.0365$, $R_{gs} = 0.000\,323$, and $R_{go} = 1.04 \times 10^{-6}$, it is found that main source of reflectance comes from the outer interface of glass and air within less than 1% error. Thus, at the scattering angle of θ, the observed scattering intensity $I(\theta)_{obs}$ can be given as the sum of two terms of $I(\theta)$ and $I(180 - \theta)$

$$I(q)_{obs} = I(\theta) + C_R R_{ga} I(180 - \theta) \qquad (7)$$

where $R_{ga}I(180 - \theta)$ is the theoretical maximum scattered intensity originated from the backward reflected beam at the scattering angle θ and C_R is defined as the fraction of the scattered light received effectively by the detector system. The value of C_R will be approximately solvent-independent and should be determined experimentally. Thus, we have tried to investigate how much the backward reflected beam from the interface of glass−air contributes to the scattering intensity especially at high scattering angle (e.g. 130°). First, a time correlation function (TCF) is measured at scattering angle 50° for the purpose of comparison. As shown in Figure 8, the linear TCF of scattering angle 50° strongly supports again that these particles are nearly monodisperse, but for the TCF of scattering angle 130°, the deviation from linearity occurs at $\tau\langle\Gamma\rangle \sim 1.5$. For TCF analysis of high scattering angle, the double exponential fitting regression is applied and then the ratio of two Γ's is obtained as 4.71, which shows very good agreement with the estimated value ($=\sin^2 65°/\sin^2 25° = 4.60$) from original and backward scattering angles. On the basis of this result, we can ensure that there should exist some contribution of the back reflection part in all TCF's. Next, to estimate the exact contribution of the reflected beam to the scattering intensity, the coefficient values of two exponential terms are compared and then the intensity of lower Γ part (i.e. reflected one) is found to be the order of about 6% of the original scattering term. Thus, it is clear that this correction term cannot be ignored for construction of a theoretical scattering function especially at high-q regime.

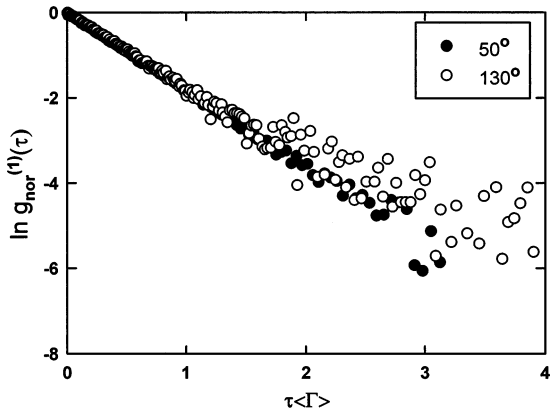

Figure 8. Semilog plot of the normalized $g_{nor}^{(1)}(\tau)$ vs $\tau\langle\Gamma\rangle$ at two different scattering angles of 50 and 130° in the PVDF/PC system. Through the regression analysis with double exponential function, it is found that the time correlation function at a scattering angle of 130° consists of two components. One is the original scattering component ($\theta = 130°$), and the other is the backward lower scattering component (i.e. $180 - \theta = 50°$) of which relative intensity is obtained on the order of 6% of the original one.

As the second correction, a finite size distribution of core radius must be introduced to set up a realistic theoretical scattering pattern, because instead of a sharp minimum of monodisperse sphere, a blunt (even flat) minimum shape is disclosed. Here some prior knowledge for the distribution of size can be approximately obtained from the q range of the blunt (or flat) part in experimental $P(q)$. After regression process, the core size distribution in PVDF/PC in the inserted graph of Figure 1 appears to be much narrower than that of PVDF/BL of Figure 2. Next even though very narrow size distribution of outside radius (i.e. R_H) is shown from the dynamic light scattering, the effect of this distribution is also taken into account for calculation of $P(q)$. For a given core size, the outside radius is automatically assigned using the linear equation giving 1:1 correspondence between two different size ranges of two independent distributions of R_H and R_1. To get the best fitting result between our experimental $P(q)$ and the theoretical one, there are three adjustable variables such as the core size distribution, the density ratio of shell part to core part, x, and the degree of contribution of the reflected beam, C_R. As shown with a solid line in Figures 1 and 2, some reasonable fitting results are obtained with $x = 0.07$ and $C_R = 0.1$ for

PVDF/PC and $x = 0.15$ and $C_R = 0.1$ for PVDF/BL, respectively, as well as with R_1's core size distribution. Without any difficulty, even the flat scattering pattern of PVDF/BL system can be generated with the relatively larger x value of 0.15 and somewhat broader distribution of core size compared with that of PVDF/PC system. The unexpectedly small value of $C_R = 0.1$ means that only 10% of total reflected beam (i.e. only 0.37% of the forward main beam intensity) contributes to the component of backward scattering angle $180 - \theta$ and such a small contribution may be attributed to mismatching of the reflected beam path with the original one. Next, using the core−shell model and fitting parameters, the relative intensity ratio of backward scattering component to the original is finally estimated on the order of 7.5% at $\theta = 130°$. This is acceptable when compared with 6% obtained from a double exponential fitting process of TCF.

Here maybe some questions will arise. Why are the dangling ends more soluble than the densely aggregated core chains? And what is the driving force? According to Wilson's reports,[29,30] a mesophase was observed in a series of fluorinated esters even where the fluoroalkyl mesogenic unit was very short (4 carbons in length) and it appeared that there was a greater driving force for segregation into an ordered or layered mesophase than in other nonfluorinated compounds. Thus on the basis of his observation, it can be assumed in our experiment of very dilute concentration that four consecutive sequences of head-to-tails may play a part as a driving force for aggregation compared to a randomly mixed sequence of head-to-tail and head-to-head (or tail-to-tail). As a result of the heptad (i.e. 7 elements) analysis in ^{19}F NMR spectra,[31] it has been found that the A7 sequence[31] (=0101010; hereafter head and tail are represented by 1 and 0, respectively) of our sample reaches to about 81% probability but B7 (=0101011), C7 (=1001010), and E7 (=0101100) have 5.0%, 4.8%, and 4.6%, respectively. We dare say that the core may consist mainly of the isoregic part like the A7 sequence and the shell of irregularly mixed sequences. As the random sequence part of shell has more entropy in thermodynamics, thus it is reasonable that this part will be more soluble in solvent than the isoregic part of core. It can be accepted that the phase of the core is probably to some extent a small-scaled ordered one but it is absolutely not the crystalline phase because of no change of its size even above the melting temperature. At this moment it is worthy to note that there is very small but some possibility about the existence of large scale of ordered phase in the core. According to Aragon and Pecora's calculation,[32] even if the large ordered phases are oriented both symmetrically and radially from the center of sphere, the depolarized scattering intensity becomes, in this particular case, undetectably weak just like our experimental result. Especially for the latter one, it had already been proved. Thus, our overall answer can be found from the core−shell type structure where the dangling polymer chains of the shell part are causing steric stabilization due to the contribution of entropy.[33] With the typical values of R_1, x, and R_H of the PVDF/PC system, a schematic diagram of core−shell structure is shown in Figure 9.

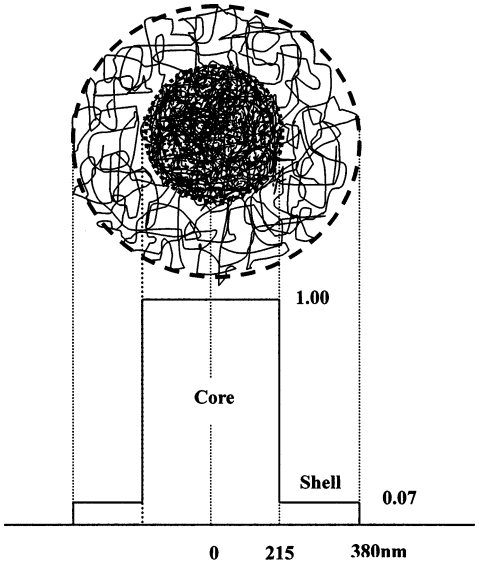

Figure 9. Schematic diagram of the core−shell structure in the PVDF/PC system. Here the core radius and the relative density are described as $R_1 = 215$ nm and $x = 0.07$, respectively.

Conclusions

By means of laser light scattering we have investigated the size and structure of PVDF aggregates at the dilute concentration regime. Even if our concentrations are much lower than the gel formation concentration, polymer chains in a pregel state cannot exist as freely separated chains in solution but as very large and monodisperse aggregate particles. Our experimental results shows that the effective hydrodynamic radii ($R_H \sim 380$ nm for PC solution, $R_H \sim 320$ nm for BL solution) and the static radius of gyration ($R_G \sim 220$ nm for both systems) keep constant for the wide temperature range of 25−160 °C. To explain such big values of $R_H/R_G = 1.45-1.8$, the core−shell model is suggested, and then the core radius and the density ratio are around $R_1 = 215 \pm 25$ nm and $x = 0.07$ for PC solution. For BL solution, they are observed as $R_1 = 190 \pm 40$ nm and $x = 0.15$. The chain conformation in the core is regarded as neither crystalline nor a well-oriented state because of no observation of a VH component in static light scattering.

It has been also discussed what is the driving force and how the structure of the aggregate develops in dilute solution. At this moment an exact mechanism is not known yet, but one suggestion is proposed: (i) There may be an attractive inter-/intramolecular force between four consecutive head-to-tail sequences in CF_2 groups of PVDF chain. (ii) The detailed structure of the core−shell model seems to be related with the relative mole ratio of irregular, head-to-head configuration to head-to-tail configuration. And also the chemical structure of solvent controls its magnitude to a certain extent and finally determines the overall structure of the core−shell. As an experimental basis of such a proposition, we mention the primitive results of light scattering for two different PVDF samples. In the second system of PVDF/PC having almost the same irregularity (mole ratio of head-to-head configuration; ∼6.0%) but low molecular weight (nominal MW = 350 kg/mol; Polyscience), it is found that almost the same size ($R_G \sim 220$ nm, $R_H \sim 390$ nm) is obtained in PC solution. However, for the third PVDF sample with a little lower irregularity of head-to-head (∼5.2%) but low MW (nominal MW = 180 kg/mol; Aldrich), much bigger aggregates of $R_H \sim 500$ nm have formed. Thus, the aggregation process

seems to be very sensitive to the amount of head-to-head configuration in the PVDF chain.

Therefore, observation of the core−shell structure in dilute solution provides an important clue for better understanding of gel morphology. Since white powders (or pellets) of PVDF quickly dissolved in our good solvent but finally appeared as the aggregate form, we believe that there should exist a kind of critical aggregation concentration like a surfactant. In the future our experiments will focus on investigation of this critical aggregation concentration and transformation of core−shell structure into a 3-dimensional gel structure near the gel point.

Acknowledgment. This research work was financially supported by the Research Fund of Kumoh National Institute of Technology in 2003.

References and Notes

(1) Guenet, J. M. *Thermoreversible Gelation of Polymers and Biopolymers*; Academic Press: New York, 1992.
(2) Stauffer, D.; Coniglio, A.; Adam, M. *Adv. Polym. Sci.* **1982**, *44*, 103−158.
(3) Tanaka, F. *Macromolecules* **1989**, *22*, 1988−1944.
(4) Nishinari, K.; Koide, S.; Williams, P. A.; Phillips, G. O. *J. Phys. (Paris)* **1990**, *51*, 1759−1768.
(5) Tanaka, F.; Stockmayer, W. H. *Macromolecules* **1994**, *27*, 3943−3954.
(6) Tanaka, F. *Macromolecules* **1998**, *31*, 384−393.
(7) Semenov, A. N.; Rubinstein, M. *Macromolecules* **1998**, *31*, 1373−1385.
(8) Rubinstein, M.; Semenov, A. N. *Macromolecules* **1998**, *31*, 1386−1397.
(9) Cho, J. W.; Song, H. Y.; Kim, S. Y. *Polymer* **1993**, *34*, 1024−1027.
(10) Mal, S.; Maiti, P.; Nandi, A. K. *Macromolecules* **1995**, *28*, 2371−2376.
(11) Dikshit, A. K.; Nandi, A. K. *Macromolecules* **1998**, *31*, 8886−8892.
(12) Mal, S.; Nandi, A. K. *Polymer* **1998**, *39*, 6301−6307.
(13) Mal, S.; Nandi, A. K. *Langmuir* **1998**, *14*, 2238−2244.
(14) Mal, S.; Nandi, A. K. *Macromol. Chem. Phys.* **1999**, *200*, 1074−1079.
(15) Park, I. H. *Polymer (Korea)* **2002**, *26*, 227−236.
(16) Kim, Y. C. Master's Degree Thesis, Kumoh National Institute of Technology, Korea, 2003.
(17) Koppel, D. E. *J. Chem. Phys.* **1972**, *57*, 4814−4820.
(18) Brown, W. *Dynamic Light Scattering. The method and some applications*; Clarendon Press: Oxford, U.K., 1993; Chapters 6 and 8.
(19) Kim, B. S.; Song, K. W.; Park, I. H.; Lee, J. O. *Proceedings of 1999 Pusan-Kyeongnam/Kyushu-Seibu Joint Symposium on High Polymers and Fibers*; Gyeongsang National University: Chinju, Korea, 1999; p 135.
(20) Huglin, M. B. *Light Scattering from Polymer Solution*; Academic Press: New York, 1972; Chapters 3 and 7.
(21) Guinier, A.; Fournet, G. *Small Angle Scattering of X-rays*; John Wiley: New York, 1955; Chapter 2.
(22) Higgins, J. S.; Benoit, H. C. *Polymers and Neutron Scattering*; Clarendon Press: Oxford, U.K., 1994; Chapter 6.
(23) Roe, R. J. *Methods of X-ray and Neutron Scattering in Polymer Science*; Oxford University Press: Oxford, U.K., 2000; Chapter 5.
(24) Grabowski, E. F.; Morrison, I. D. In *Measurement of Suspended Particles by Quasi-elastic Light Scattering*; Dahneke, B. E., Ed.; John Wiley: New York, 1983; pp 199−236.
(25) Burchard, W. *Adv. Polym. Sci.* **1983**, *48*, 1−124.
(26) Park, S.; Chang, T.; Park, I. H. *Macromolecules* **1991**, *24*, 5729−5731.
(27) Berne, B. J.; Pecora, R. *Dynamic Light Scattering with Applications to Chemistry, Biology and Physics*; John Wiley: New York, 1976.
(28) Hirzinger, B.; Helmstedt, M.; Stejskal, J. *Polymer* **2000**, *41*, 2883−2891.
(29) Wilson, L. M. *Macromolecules* **1995**, *28*, 325−330.
(30) Wilson, L. M.; Griffin, A. C. *Macromolecules* **1994**, *27*, 1928−1931.
(31) Cais, R. E.; Sloane, N. J. *Polymer* **1983**, *24*, 179−187.
(32) Aragon, S. R.; Pecora, R. *J. Colloid Interface Sci.* **1982**, *89*, 170−184.
(33) Napper, D. H. *Polymeric Stabilization of Colloidal Dispersions, Colloid Science*; Academic Press: London, 1983; Vol. 3.
(34) Cheng, L.-P.; Young, T.-H.; Fang, L.; Gau, J.-J. *Polymer* **1999**, *40*, 2395−2403.

MA030534V